SPECTRAL AND THERMAL STUDIES OF SOME 4-(*O*-ACETYL)GLYCOPYRANOSYLAMINOPYRIMIDINE DERIVATIVES

R. LÓPEZ GARZÓN *, A. SÁNCHEZ RODRIGO, M. NOGUERAS MONTIEL
and J. NEGRILLO PÉREZ

Departments of General and Organic Chemistry, University College, 23071 Jaén (Spain)

A.M. BERNALTE GARCÍA and C. VALENZUELA CALAHORRO

Department of Inorganic Chemistry, University of Extremadura, Badajoz (Spain)

(Received 4 June 1985)

ABSTRACT

A spectral study (IR and UV spectroscopies) of seven 4-(*O*-acetyl)glycopyranosyl-aminopyrimidine derivatives has been carried out. The thermal study of the compounds allowed us to characterize the following processes: (i) desolvations, (ii) solid–solid transitions, (iii) melting, (iv) pyrolytic decompositions. Through the IR spectral study it was established that pyrolytic decompositions of all the compounds start with the acetyl groups. The reaction orders and activation energies of the deacetylation processes have been calculated.

INTRODUCTION

Extensive literature exists about the biological role of pyrimidines and their nucleosides [1–5]. Moreover, some metal complexes of the above-mentioned compounds have also received great interest because of their activity in biological processes [3,6].
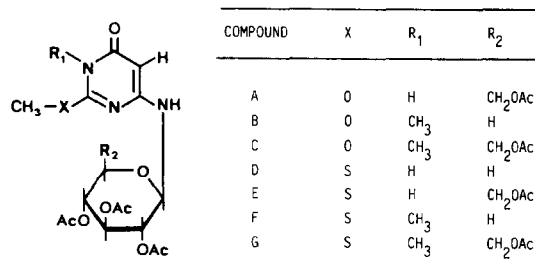
In two recent papers, the spectral (IR and UV–visible) and thermal study of two series of pyrimidine derivatives (six 4-glycopyranosylamino-5-nitroso-6-oxopyrimidine derivatives [7] and seven 4-glycopyranosylamino-6-oxopyrimidine derivatives [8]) was reported in order to complete their characterization. Recently, we synthesized and characterized some metal complexes (Pd(II) and Au(III)) of four of the 4-glycopyranosylamino-5-nitroso-6-oxopyrimidine derivative compounds [9].

In this paper we complete the spectral characterization [10] and carry out

_____
* To whom correspondence should be addressed.

the thermal study of the 4-(O-acetyl)glycopyranosylaminopyrimidine derivatives given in Scheme 1.

COMPOUND	X	R$_1$	R$_2$
A	O	H	CH$_2$OAc
B	O	CH$_3$	H
C	O	CH$_3$	CH$_2$OAc
D	S	H	H
E	S	H	CH$_2$OAc
F	S	CH$_3$	H
G	S	CH$_3$	CH$_2$OAc

Scheme 1

EXPERIMENTAL

The seven compounds under study were synthesized and purified as previously reported [10].

To characterize the compounds obtained we employed ^{1}H-NMR spectroscopy using a Hitachi/Perkin–Elmer R-600 FT-NMR spectrometer, DMSO-d_6 and Cl$_3$CD as solvents and TMS as internal standard.

The analyses of the compounds were realized at the National Institute of Organic Chemistry (C.S.I.C., Madrid). The analytical and yield data obtained, and also the formulae, are listed in Table 1.

The infrared (4000–200 cm^{-1}) spectra were recorded in KBr pellets, in a Beckman 4250 spectrophotometer. UV spectra (400–200 cm^{-1}) were recorded in a Beckman 25 spectrophotometer, using H$_2$O as solvent.

DSC plots were obtained with a Mettler DSC-20 differential scanning calorimeter at a heating rate of 5°C min^{-1}, using samples of 1.35–1.97 mg. Thermogravimetric curves were obtained in a Mettler TG 50 thermobalance, in a static, pure air atmosphere, at a heating rate of 10°C min^{-1}, with samples of 8.71–11.13 mg.

TABLE 1

Analytical and yield data

Compound	%C	%H	%N	Formula	Yield (%)
A·H$_2$O	46.62 (46.17)	5.52 (5.27)	8.59 (8.42)	C$_{19}$H$_{25}$N$_3$O$_{11}$·H$_2$O	64
B·H$_2$O	46.50 (46.85)	5.83 (5.74)	9.80 (9.65)	C$_{17}$H$_{23}$N$_3$O$_9$·H$_2$O	53
C	49.48 (49.62)	5.61 (5.51)	8.66 (8.58)	C$_{20}$H$_{27}$N$_3$O$_{11}$	89
D·C$_2$H$_6$O	46.26 (46.85)	5.81 (5.86)	9.30 (9.11)	C$_{16}$H$_{21}$N$_3$O$_8$S·C$_2$H$_6$O	60
E·H$_2$O	45.24 (45.15)	5.17 (4.95)	8.30 (8.32)	C$_{19}$H$_{25}$N$_3$O$_{10}$S·H$_2$O	98
F	47.54 (47.18)	5.40 (5.35)	9.78 (9.70)	C$_{17}$H$_{23}$N$_3$O$_8$S	42
G	47.89 (48.20)	5.43 (5.51)	8.38 (8.35)	C$_{20}$H$_{27}$N$_3$O$_{10}$S	50

The analytical data in parentheses are theoretical values.

RESULTS AND DISCUSSION

Spectral study

The most significant bands of the IR spectra and their tentative assignments are given in Table 2.

On comparing these data with the IR spectral assignments of the respective non-acetylated compounds [8] it can be seen that all the characteristic bands of the non-acetylated compounds (both those assigned to the pyrimidinic cycles and the pyranosic residues) are present in the IR spectra of the respective acetyl derivative; with the exception of the ν(O–H) stretching vibration, which appears only in the IR spectrum of D due to the OH group of one ethanol molecule, as will be discussed later. Likewise, the bands attributed by Nakanishi and Solomon [11] to the pyranosic ring have been assigned here too.

On the other hand, all the IR spectra show one strong, generally wide band at about 1750 cm^{-1}. These bands have been assigned to ν(C=O) stretching vibration of groups added to the sugar residue. In the IR spectrum of G, this band appears to be split in two; this is probably due to a hydrogen bridge interaction between the C=O grouping of the acetate group linked to C-2′ and the N–H group substituted in C-4 of the pyrimidine ring [12]. The above interaction has not been detected in the IR spectrum of the remaining six compounds; nevertheless, the expansion of the respective bands enables us to suppose that they might include the two expected bands.

The ν(C–O) stretching vibrations due to C–O–C (acetate groups) are in the range 1200–1300 cm^{-1}. These bands are wide and strong, probably hiding the ν(C–N) stretching vibration bands.

The UV spectral data of the compounds under study are given in Table 3. As could be expected, the number and class of bands in the 200–400 cm^{-1} range are similar to those of the respective non-acetylated homologues, previously reported [13–15].

Thermal study

TG and DSC curves of the seven acetylated compounds are shown in Figs. 1 and 2, respectively. The thermal data given in Table 4 have been obtained from these figures. The study of the curves in Figs. 1 and 2 allows us to identify four classes of thermal reactions: (i) desolvations, (ii) solid–solid transitions, (iii) melting, (iv) pyrolytic decompositions.

Desolvations

In the TG plots of A, B and E, weight losses occur corresponding to one water molecule (Table 4); this is in agreement with the proposed formulae (Table 1) for these compounds. The hydration enthalpies of A and E are 53.0

TABLE 2

IR spectral data (ν, cm^{-1})

Compound	ν(N–H)	ν(O–H)	ν(C–H)	ν(C=O) [a]	ν(C=O) [b]	ν(C=N) and ν(C=C)	ν(C–N) and ν(C–O) [a]	ν(C–O)	Skeletal pyranosic ring	ν(C–S)
A·H$_2$O	3400 w		3020 w 2980 w 2940 w 2860 w	1745 s, br	1660 s, br	1610 m 1580 m	1220 s, br	1090 m 1030 m	945 w 900 w 750 w	
B·H$_2$O	3390 m, br		2900 w	1740 s	1630 s	1590 s 1525 m	1230 s 1205 s	1055 m 1035 m	930 w 770 w	
C	3370 w, do		2960 w 2940 w	1745 s, br	1685–1665 s, br	1620 m 1560 s	1280 m 1255 s 1230 s 1210 s	1085 m 1030 s	935 w 900 w 795 w	
D·C$_2$H$_6$O	3370 w, br	3260 w	3030 w 2940 w 2860 w	1755 s	1650 s, br	1600 m 1545 m, br	1245 s 1220 s	1065 m 1030 m	905 w 875 w 810 w	600 w
E·H$_2$O	3420 w		3030 w 2950 w 2870 w	1750 s, br	1660 s, br	1590 m 1525 m, br	1225 s, br	1030 s	960 w 900 w 800 w	600 w
F	3340 m		3010 w 2980 w 2930 w 2870 w	1750 s	1670 s	1600 m 1520 s, br	1245 s 1220 s	1090 m 1065 s 1030 s	930 w 870 w 760 w	600 w
G	3400 w, do		3010 w 2930 w	1750 s 1725 s	1670 s	1600 m 1515 s	1230 s 1210 s	1085 m 1065 m 1055 m 1020 s	960 w 895 w 765 w	590 w

[a] Acetate groups. [b] 6-Oxo group.
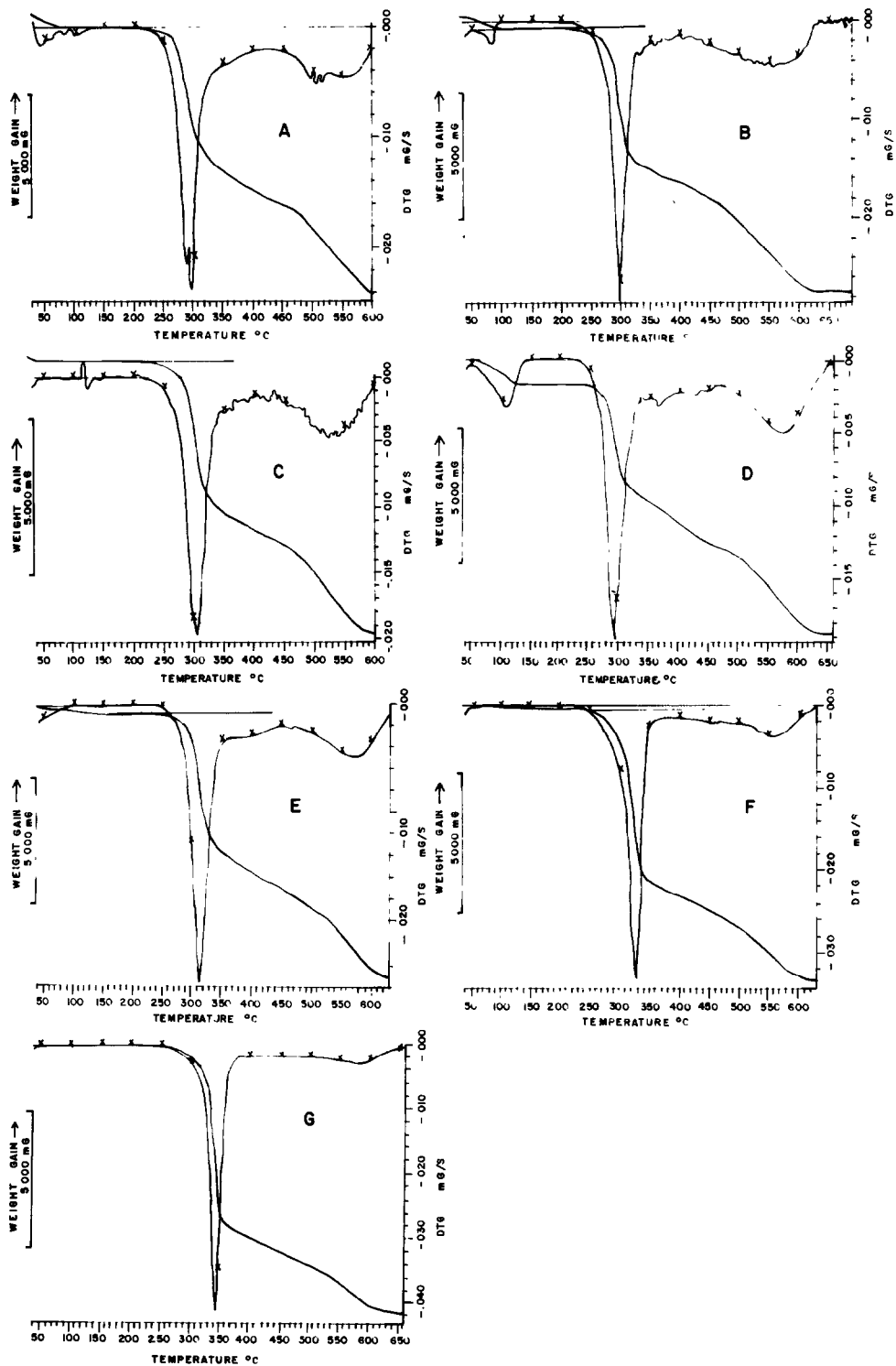
w, weak; m, medium; s, strong; br, broad; do, double.
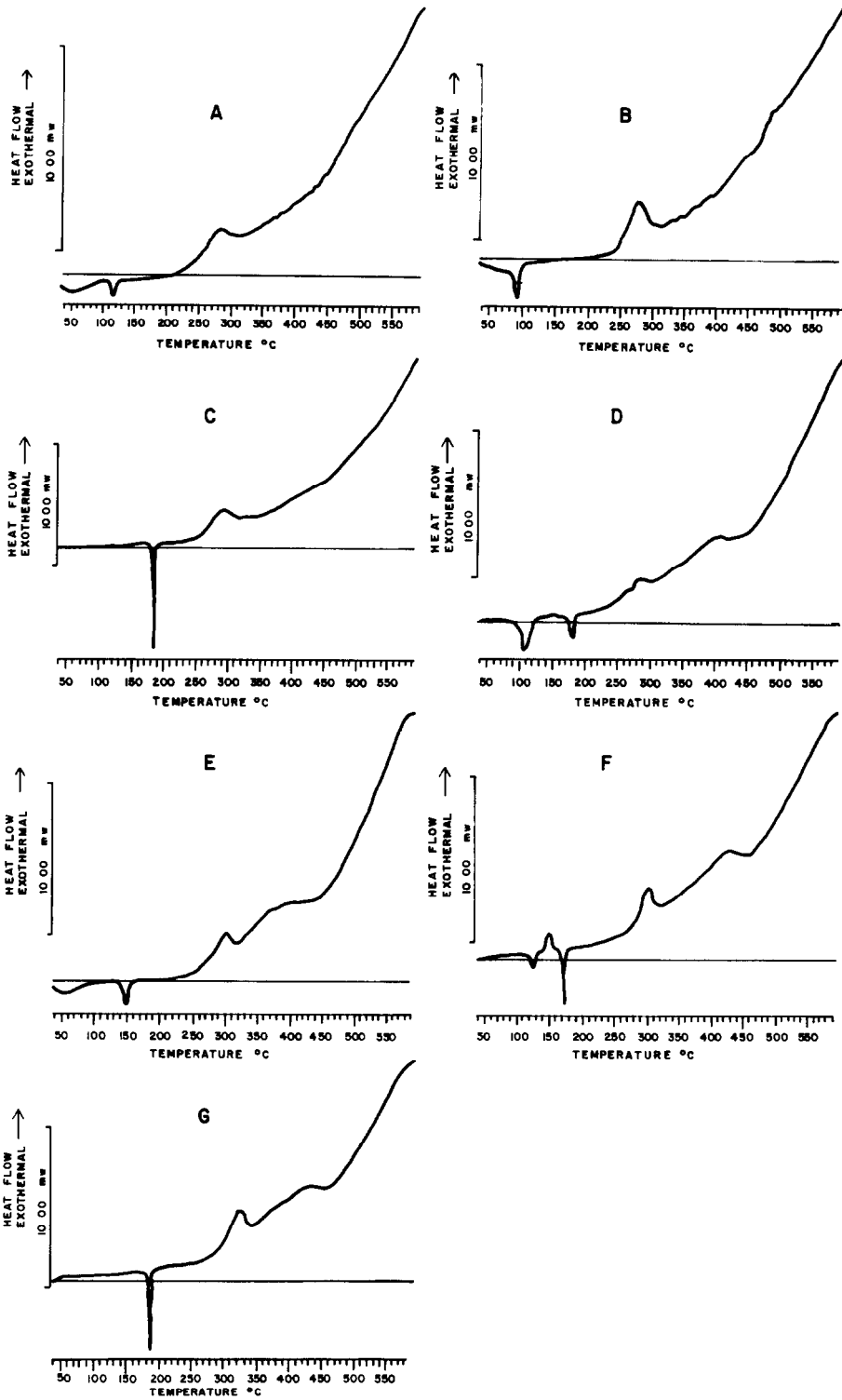
Fig. 1. TG curves.

64

Fig. 2. DSC curves.

TABLE 3

UV spectral data in aqueous solution

Compound	Concentration (mol l^{-1})	λ_{max} (nm)	ϵ	Assignments
A·H$_2$O	4.88×10^{-5}	211	27600	$\pi - \pi^*$
		266	16500	$n - \pi^*$
B·H$_2$O		213		$\pi - \pi^*$
		266		$n - \pi^*$
C	5.97×10^{-5}	213	29900	$\pi - \pi^*$
		266	15000	$n - \pi^*$
D·C$_2$H$_6$O	5.06×10^{-5}	216	22000	$\pi - \pi^*$
		236	19600	$\pi - \pi^*$
		280	9200	$n - \pi^*$
E·H$_2$O	5.13×10^{-5}	216	23000	$\pi - \pi^*$
		236	20000	$\pi - \pi^*$
		280	9600	$n - \pi^*$
F	4.19×10^{-5}	219	23400	$\pi - \pi^*$
		234	21800	$\pi - \pi^*$
		281	8300	$n - \pi^*$
G	4.39×10^{-5}	219	29100	$\pi - \pi^*$
		234·	26900	$\pi - \pi^*$
		281	10400	$n - \pi^*$

and 57.0 kJ mol^{-1}, respectively; the high values indicate that the water molecules are probably linked to the corresponding organic molecules via a hydrogen bridge. The enthalpy of dehydration could not be calculated for compound B because the corresponding endotherm overlaps with that of its melting.

The TG curve of D shows a weight loss (9.99%) in the temperature range 70–120°C. An endothermic effect, starting at 80°C and finishing at 130°C (peak at 110°C), accompanies the process ($\Delta H = 36.94$ kJ mol^{-1}). The calculated percentage corresponding to one ethanol molecule is 9.98%, which is in good agreement with the above value.

The existence of an ethanol crystallization molecule is not surprising if we consider that this compound was recrystallized in an ethanolic medium. Nevertheless, to corroborate this it was verified that the ^{1}H-NMR spectrum of D shows a triplet signal, centered at 0.65 ppm, corresponding to one ethanol molecule for one unsolvated molecule of D.

In the IR spectrum of the sample remaining after heating D at 145°C, the band assigned at ν(O–H) does not appear; besides, the band corresponding to ν(N–H) is shifted to a higher wavenumber. This may indicate some interaction between C$_2$H$_6$O and the pyrimidine derivative via a hydrogen bridge.

Solid–solid transitions

The DSC plot of F presents one endothermic effect, with a minimum at 127°C, followed by an exothermic effect, centered at 150°C (see Fig. 2); no

TABLE 4

TG and DSC data

Compound	Desolvations			Solid–solid transitions	
	T (°C)	wt. loss (%)	ΔH (kJ mol^{-1})	T (°C)	ΔH (kJ mol^{-1})
A·H$_2$O	53	3.80 (3.78) [c]	53.0		
B·H$_2$O		4.30 (4.17) [c]			
C					
D·C$_2$H$_6$O	110	9.99 (9.98) [c]	36.9		
E·H$_2$O	57	3.20 (3.57) [c]	57.0	127, endo	13.3
				150, exo	−20.4
F					
G					

[a] Temperature at the peak of the endotherm.
[b] Melting temperature measured in a capillary.
[c] Theoretical values.
[d] This value includes the desolvation enthalpy.

variations in weight are observed in the corresponding TG curve (Fig. 1). Moreover, it was proved that the sample does not fuse at the above-cited temperatures. Also, we arrested the species at 160°C and cooled it; on heating again, after 2 h, no noticeable thermal effects were observed in the DSC plot. Two samples of F were heated at 135 and 160°C, respectively, and after 2 h their IR spectra were registered, both being equal. They differ from the IR spectrum of unheated F only in the fact that a singlet (unassigned) band, of medium intensity, at 1440 cm^{-1}, splits in two on heating.

All these features enable us to suppose that the two effects cited above arise from some probable change in crystal structure, which is accompanied by a net loss of heat of 7.1 kJ mol^{-1}.

Melting

All the compounds under study present defined melting processes below

TABLE 5

Kinetic data for the deacetylation processes

Compound	Temperature (°C) and thermal effects	E_A (kJ mol^{-1})	n
A·H$_2$O	275, exo	71.9	1.05
B·H$_2$O	277, exo	76.3	0.97
C	290, exo	73.2	0.86
D·C$_2$H$_6$O	287, exo	41.1	0.27
E·H$_2$O	302, exo	71.0	0.75
F	305, exo	81.7	0.66
G	321, exo	71.1	0.52

Melting		Deacetylation		Other effects	
T (°C) [a]	ΔH (kJ mol^{-1})	T (°C)	ΔH (kJ mol^{-1})	T(°C)	ΔH (kJ mol^{-1})
118.0 (130) [b]	9.76	275, exo	−112.2	450 w, exo	
(90) [b]	70.32 [d]	277, exo	−115.8	490 w, exo	
184.0 (182) [b]	41.46	290, exo	−143.7	490 w, exo	
216.0 (200) [b]	33.20	287, exo	−26.04	391, exo	−46.10
149.0 (139) [b]	21.74	302, exo	−70.53	358, exo	−99.34
				590, exo	−1244.65
172.0 (169) [b]	22.41	305, exo	−114.29	404, exo	−135.03
187.0 (180) [b]	38.71	321, exo	−182.03	400, exo	−150.23

their respective temperature of pyrolytic decomposition. On the other hand, the melting temperature values are largely lower than those of their non-acetylated homologues [8]; this fact may indicate strong interactions between the unacetylated molecules in which the OH groups of the sugar residues play an important role. Thus, the relatively low values of melting temperatures in the compounds studied in this work point to relatively weak molecular interactions.

The endothermic effects corresponding to these processes appear in the respective DSC plots and from them, the fusion enthalpies have been calculated (see Table 4).

Pyrolytic decompositions

All the compounds are relatively stable in the liquid state, as can be seen from their DSC and TG curves.

On the other hand, the decomposition temperatures are largely lower than those of their non-acetylated homologous compounds [8]. This feature enables us to suppose that, in these compounds, the pyrolytic decomposition processes start, most probably, through the loss of the acetyl groups. To prove this, we measured from TG curves the temperature at which the weight loss, from the start of pyrolysis, was equal to that calculated for all of the acetyl groups, in each compound. The resulting temperature was the same as that of the termination of the first exothermic effect corresponding to the pyrolytic decompositions. We heated each compound at the temperature of the theoretical deacetylation, thus obtaining its IR spectrum. On comparison with that of the unheated sample, the disappearance of ν(C=O) and ν(C–O) of the acetyl groups was verified; the remaining bands appeared practically unaffected.

The reaction orders, n, and the activation energies, E_A, of the thermal reactions of deacetylation have been calculated, from TG data, by the

standard equation

$$d\alpha/dt = k(1 - \alpha)^n$$

according to which the reaction order, n, is related to the decomposition rate, α [16]. The values obtained are listed in Table 5.

All the deacetylated compounds are unstable and continue their decomposition steadily; this occurs, probably, by means of a mechanism similar to that previously described for the non-acetylated homologues [8].

From the TG curves it can be seen that abrupt weight losses follow deacetylation processes, up to about 320 (A and B) and 350°C (D, E, F and G). At these temperatures, the weight losses continue without cessation, but slowly, up to about 500°C. The decomposition processes finish in the range 600–650°C. At the final temperature no samples remain in the crucible.

New exothermic effects, in all DSC plots, appear at temperatures between 358 and 590°C. The corresponding temperatures and energies are given in Table 4.

REFERENCES

1 A. Bloch (Ed.), Chemistry Biology and Clinical Uses of Nucleosides Analogues, New York Academy of Sciences, New York, 1975.

2 R.M. Ottenbrite and G.B. Butler (Eds.), Anticancer and Interferon Agents, Vol. 24, Dekker, New York, 1984.

3 J.L. Rideout, D.W. Henry and M. Beacham (Eds.), Nucleosides Nucleotides and Their Biological Applications, Academic Press, New York, 1983.

4 C. Nakayama, H. Machida and M. Saneyoshi, J. Carbohydr. Nucleosides Nucleotides, 6 (1979) 295.

5 P.F. Torrence, G.F. Huang, M.W. Edwards, B. Bhoosnan, J. Descamps and E. Clercq, J. Med. Chem., 22 (1979) 316.

6 M.N. Hughes, The Inorganic Chemistry of Biological Processes. 2nd edn., Wiley, London, 1981.

7 A. Sánchez, Rodrigo, M. Nogueras Montiel, R. López Garzón, M.D. Gutierrez Valero and E. Colacio Rodríguez, Thermochim. Acta, in press.

8 R. López Garzón, M. Nogueras Montiel, A. Sánchez Rodrigo, J. Negrillo Pérez and A.M. Bernalte García, Thermochim. Acta, in press.

9 R. López, A. Sánchez, J. Nogueras and C. Valenzuela, Rev. Chim. Miner., submitted.

10 R. Asenjo, M. Melgarejo, C. Rodríguez, M. Nogueras and A. Sánchez, An. Quím., 79 C, (1983) 417.

11 K. Nakanishi and P. Solomon, Infrared Absorption Spectroscopy, Holden-Day, San Francisco, CA, 1977.

12 A.R. Todd, Experiment on the synthesis of purine nucleosides, Parts I–XXVII, J. Chem. Soc., (1943–1950).

13 D.J. Brown, The pyrimidines, Vol. I, Interscience, London, 1962.

14 J. Kister, D. Bourn Roubaud, L. Boucasse and J. Metzger, J. Spectrosc. Lett., 13(1) (1980) 1.

15 D. Bourn Roubaud, J. Kister, L. Boucasse and J. Metzger, J. Spectrosc. Lett., 14(6) (1981) 431.

16 M.I. Pope and M.D. Judd, Differential Thermal Analysis, Heyden, London, 1980.